EUROFUSION WPMST1-CP(16) 15302

B Labit et al.

# The physics of the heat flux narrow decay length in the TCV scrape-off layer: experiments and simulations

Preprint of Paper to be submitted for publication in
Proceedings of 26th IAEA Fusion Energy Conference

This work has been carried out within the framework of the EUROfusion Consortium and has received funding from the Euratom research and training programme 2014-2018 under grant agreement No 633053. The views and opinions expressed herein do not necessarily reflect those of the European Commission.

# The physics of the heat flux narrow decay length in the TCV scrape-off layer: experiments and simulations

B. Labit[1], F. Nespoli[1], J. Horacek[2], C. Tsui[3,1], J.A. Boedo[3], C. Theiler[1], I. Furno[1], F.D. Halpern[1], P. Ricci[1], R.A. Pitts[4], the TCV Team[5] and the EUROfusion MST1 Team[6]

[1]Swiss Plasma Center (SPC), Ecole Polytechnique Fdrale de Lausanne (EPFL), CH-1015 Lausanne, Switzerland
[2]IPP.CR, Institute of Plasma Physics AS CR, Za Slovankou 3, 182 21 Praha 8, Czech Republic
[3]University of California-San Diego, La Jolla, California 92093, USA
[4]ITER Organization, CS 90 046, 13067 St Paul Lez Durance, France
[5]See OV/P-1, this conference
[6]See OV/P-12, this conference

*Corresponding Author:* benoit.labit@epfl.ch

**Abstract:**
Heat flux profiles at the target of inboard limited L-mode plasmas are found to be characterized by two scale lengths, with steeper gradients near the separatrix. Recent experiments in TCV are revealing that the near SOL gradients disappear at large normalized resistivity ($\nu \sim 10^{-2}$), which seems to correspond to the transition from the Sheath-Limited regime to the Conduction-Limited regime in the near SOL. It is seen that the power carried by the near SOL component is strongly correlated with the amplitude of non-ambipolar currents flowing to the limiters. Nonlinear global simulations of plasma dynamics for the TCV SOL are able to reproduce the near SOL steep gradients, though its strength appears weaker than in the experiments.

## Introduction

During their start-up phase, tokamak plasmas are often limited on the inner wall, before the divertor is formed. The inner wall plasma-facing components are designed in order to sustain the deposited heat flux during this phase. The design is usually based on the assumption that the parallel heat flux $q_\parallel$, entering into the scrape-off layer (SOL) essentially at the outboard midplane, is described by an exponentially decaying profile with a characteristic decay length $\lambda_q$: $q_{\parallel,u}(r_u) = q_0 \exp(-r_u/\lambda_q)$ where $r_u = R - R_{\mathrm{LCFS}}$ is the radial coordinate at the outboard midplane SOL. Then, assuming transport along the magnetic field lines solely, the heat flux onto the first wall can be estimated and by shaping the tiles, one can sufficiently increase the wetted area and optimize the power

handling. Nevertheless, dedicated experiments in several tokamaks [1] (and references therein), including TCV [2], have demonstrated that an enhancement of the heat deposition, measured with an infrared (IR) camera, is observed in the vicinity of the contact point for inboard limited plasmas. Indeed, for all the discharges, the parallel heat flux profile, once remapped to the outboard midplane, exhibits two decay lengths with a short decay length for the near SOL $\lambda_{q,n}$ of $\sim$ few mm and a longer decay length for the far SOL $\lambda_{q,f}$ about ten times longer:

$$q_{\parallel,u}(r_u) = q_n \exp(-r_u/\lambda_{q,n}) + q_f \exp(-r_u/\lambda_{q,f}). \quad (1)$$

The extrapolation to ITER suggests this enhanced heat load could lead to a melting of the beryllium first wall panels and so the first wall panel shape has been modified to safely exhaust the heat load [1]. In TCV, the amount of power deposited onto the inner wall due to the narrow feature,

$$\Delta P_{\text{near}} = 4\pi R_{LCFS} \lambda_{q,n} q_n \frac{B_{\theta,u}}{B_{\varphi,u}}, \quad (2)$$

has been estimated, where $B_{\theta,u}$ and $B_{\varphi,u}$ are the poloidal and toroidal magnetic field at the outboard midplance, respectively. A nonlinear regression provides an empirical scaling showing that $\Delta P_{\text{near}}$ increases mainly with the electron temperature, and decreases with plasma density, current and elongation [2]. Finally, when available, direct measurements with reciprocating Langmuir probes do not systematically show evidence of steeper gradients in the near SOL at the outboard midplane [1, 3]. An explanation for the existence of the near SOL steep gradients in inboard-limited L-mode plasmas has been attempted based on the heuristic drift SOL model [4], a successful model to explain the scaling of the power width in H-mode plasmas [5].

Those results have motivated additional experiments in TCV. In particular, one would like to address the following open questions: firstly, on a pragmatic level, can experimental conditions for which the near SOL feature is not observed be found? Secondly, can experimental data and numerical simulations give some insights on the underlying physical mechanism at the origin of the steep gradients in the near SOL?

## Experimental setup

The TCV tokamak ($R = 0.88$ m, $B_T < 1.5$ T, $I_p < 1$ MA) is a full carbon device and was principally designed to investigate the physics of strongly shaped plasmas ($1 < \kappa < 1.6$, $-0.4 < \delta < 0.4$). Its inner wall is continuous consisting of $32 \times 7$ graphite tiles in the toroidal and vertical directions, respectively. The main diagnostic to measure target heat loads is a recently installed infrared (IR) camera, mounted on a lateral port and monitoring the temperature of the graphite tiles of a portion of the central column. The detector (320 pixels $\times$ 256 pixels) is sensitive, with a spectral filter, to radiation in the wavelength range from 4 to 5 $\mu$m. The acquisition rate and the spatial resolution are 200 Hz and 1.6 mm/pixel in full frame using a 12.5 mm focal-length lens [7]. The FOV covers approximately 3 tiles in both directions and determines the portion of the SOL which can be investigated, in particular it defines the maximum value

for $r_u$. In addition to the IR camera, the central column is equipped with an array of flush-mounted Langmuir probes (LPs) (Fig.1). For the experiments reported here, every two probes are configured to measure the floating potential $V_{fl}$ while the others are negatively biased and measure the ion saturation current $I_{sat}$ at 200 kHz. Edge electron density and temperature are provided by Thomson scattering measurements. In addition, SOL parameters at the outboard midplane are measured by a recently installed 10 tip reciprocating probe [8]. It allows measurements of the ion saturation current, floating potential, Mach number and electron temperature and their fluctuations.

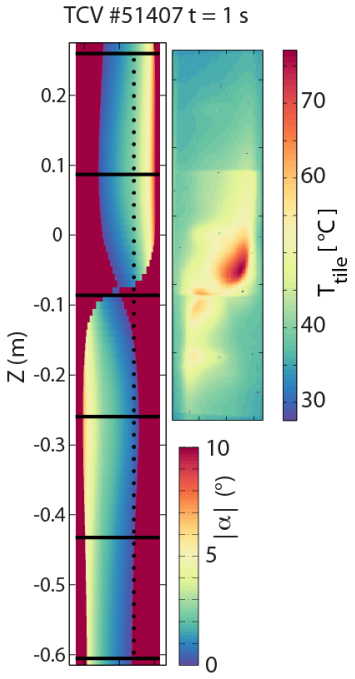


*FIG. 1: (left) Angle between the tile surface and the magnetic field. Wall shadowed regions are shown in dark red. Black dots indicate the LP location; (right) Measured temperature on three tiles of the TCV inner wall.*

Infrared images are converted into a 2D temperature profile $T_{tile}(R\varphi, Z)$. The THEODOR code [9], which solves the heat diffusion equation, is used to compute the heat flux deposited onto the tiles $q_{dep}(R\varphi, Z)$. Since the inner wall tiles are shaped [6], the angle $\alpha(R\varphi, Z)$ between the magnetic field and the tile surface varies in the toroidal and vertical directions. Using the reconstructed magnetic equilibrium, each point of the tile surface is converted from the real space coordinates $(R\varphi, Z)$ to the upstream coordinates $r_u$. The target heat flux $q_{dep}(r_u, \alpha)$ is decomposed as follows:

$$q_{dep}(r_u, \alpha) = q_{\parallel,t}(r_u)\sin\alpha + q_{\perp,t}(r_u)\cos\alpha + q_{BG}, \qquad (3)$$

where $q_{\parallel,t}$ is the target heat flux parallel to the magnetic field, $q_{\perp,t}$ is the target cross-field heat flux and $q_{BG}$ is a background heat flux. The last two quantities are estimated with an exponential fit of the deposited heat flux at grazing angle, $q_{dep}(r_u, \alpha = 0) = q_{\perp,t}(r_u) + q_{BG} = q_{\perp,0}\exp(-r_u/\lambda_\perp) + q_{BG}$. Finally, the parallel heat flux at the target $q_{\parallel,t}(r_u)$ is projected upstream: $q_{\parallel,u}(r_u) = \frac{B_{tot,u}}{B_{tot,t}} q_{\parallel,t}(r_u)$ which is fitted with Eq.1.

## Experimental evidences for near SOL suppression

The scaling, proposed in [2], for the strength of the narrow SOL suggests that $\Delta P_{near}$ is inversely proportional to the normalized Spitzer resistivity

$$\Delta P_{near} \propto \nu^{-1} \quad \text{with} \quad \nu = \frac{e n_{e,0} R_0 \eta_\parallel}{m_i c_{s,0}} \propto n_{e,0} T_{e,0}^{-3/2}, \qquad (4)$$

where $n_{e,0}$ is the plasma density at the LCFS, $R_0$ is the major radius of the plasma, $m_i$ is the ion mass, $c_{s,0}$ is the ion sound speed at the LCFS and $\eta_\parallel$ is the Spitzer resistivity. For a given shape ($\kappa = 1.4$ and $\delta = 0$), two scans are performed for inboard limited L-mode plasmas in deuterium: the plasma current $I_p$ is varied from 85 kA to 210 kA at a fixed density ($n_{e,av} = 2.3 \times 10^{19}\, m^{-3}$) and, in the second scan, the averaged plasma density $n_{e,av}$ is changed from $1 \times 10^{19}\, m^{-3}$ to $3.3 \times 10^{19}\, m^{-3}$ at fixed plasma current $I_p$=140 kA.

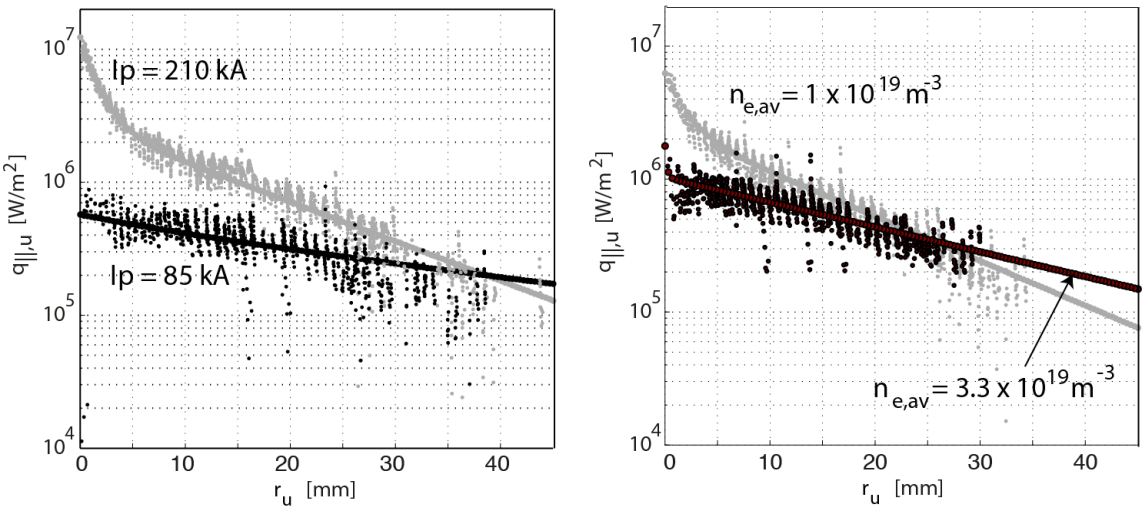


*FIG. 2: Target parallel heat flux profiles mapped to the outboard midplane for inboard limited plasmas (left) for $I_p$=210 kA (gray) and $I_p$ = 85 kA (black) at $n_{e,av,19} \simeq 1.7\,m^{-3}$; (right) for $n_{e,av,19} = 1\,m^{-3}$ (gray) and for $n_{e,av,19} = 3.3\,m^{-3}$ (black) at $I_p$=140 kA.*

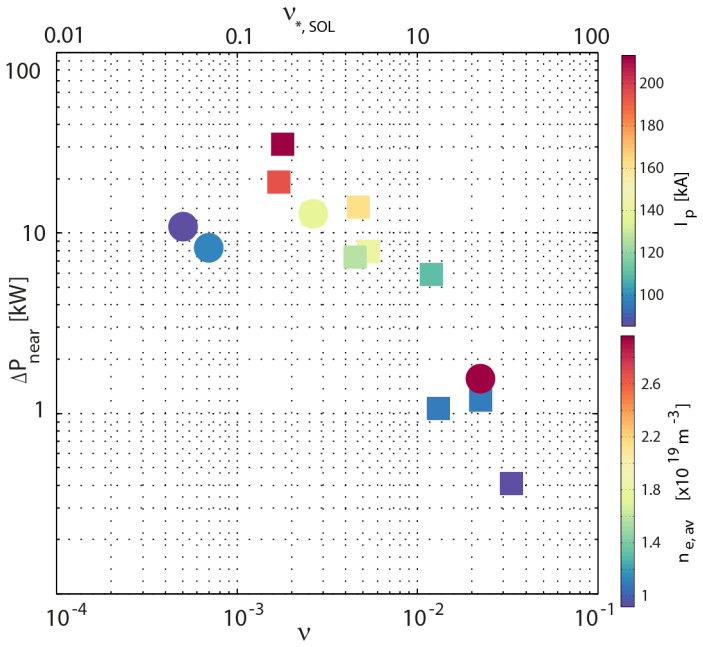


*FIG. 3: Power in the near SOL $\Delta P_{near}$ as a function of normalized Spitzer collisionality $\nu$ and the normalized SOL collisionality $\nu_{\star,SOL}$ for the $I_p$ scan (□) and the density scan (◯).*

The parallel heat flux profiles mapped to the outboard midplane are shown in Fig. 2 for the extreme values in both scans. While at large $I_p$ or low $n_{e,av}$, the near SOL steep gradient is clearly visible and $q_{\parallel,u}$ profiles are well fitted by Eq.1, the near SOL component disappears at low plasma current or high density. To our knowledge, this is the first time that experimental evidence is reported for the absence of strong gradients in the near SOL. Results from both scans are summarized in Fig.3 where the power in the near SOL $\Delta P_{near}$ is plotted as a function of the normalized Spitzer resistivity $\nu \simeq 10^{-3}\nu_{\star,SOL}$. $\Delta P_{near}$ monotically decreases with $\nu$ and for $\nu \gtrsim 10^{-2}$, steep gradients in the near SOL are not observed. In fact, the near SOL steep gradients disappear when the SOL makes the transition from the Sheath-Limited regime to the Conduction-Limited regime, characterized by high recycling and large temperature gradients along the magnetic field lines. This regime is attained

when $\nu_{\star,SOL} \gtrsim 15$ with $\nu_{\star,SOL} \simeq 10^{-16} L_{\parallel} n_{e,u} T_{e,u}^{-2}$ where $L_{\parallel}$ is the connection length from outboard midplane to the target [10]. This might have some implications for the start-up phase of a tokamak plasma, namely that the plasma has to be resistive enough during the limited phase before the formation of the divertor to be safe with the power exhaust on the inner wall. Estimates for ITER [3] give $10^{-3} < \nu_{ITER} < 10^{-2}$ suggesting that steep gradients in the near SOL will be present.

## Correlation between non-ambipolar currents and near SOL

On COMPASS, the potential role of non-ambipolar currents, i.e currents involving more charges of one sign than of the opposite sign, at the origin of near SOL steep gradients has been investigated [11]. Although non-ambipolar currents at the limiter are clearly measured in limited plasmas, their associated heat flux cannot explain the strength of the near SOL. In TCV, non-ambipolar currents are monitored with floating potential measurements on the inner wall with Langmuir probes as illustrated in Fig.4(left). At low resistivity ($I_p = 210$ kA), where the narrow SOL is present, non-ambipolar currents are measured: in the immediate vicinity of the separatrix, the floating potential is negative, meaning that a net electron current is flowing to the limiter. Further out, a net ion current flows to the limiter and the far scrape-off layer is ambipolar with $V_{fl} \simeq 0$. At large resistivity, for which the near SOL steep gradients are not seen with the IR camera, non-ambipolar currents vanish: $V_{fl}(r_u) \simeq 0$ across the entire SOL. This is the evidence that non-ambipolar currents and the appearance of the near SOL feature are indeed correlated. In Fig.4(right), the floating potential drop $\Delta V_{fl} = \max(V_{fl}(Z)) - \min(V_{fl}(Z))$ is shown as a function of the normalized Spitzer resistivity. The potential drop decreases with $\nu$ and gets close to zero for $\nu \gtrsim 10^{-2}$.

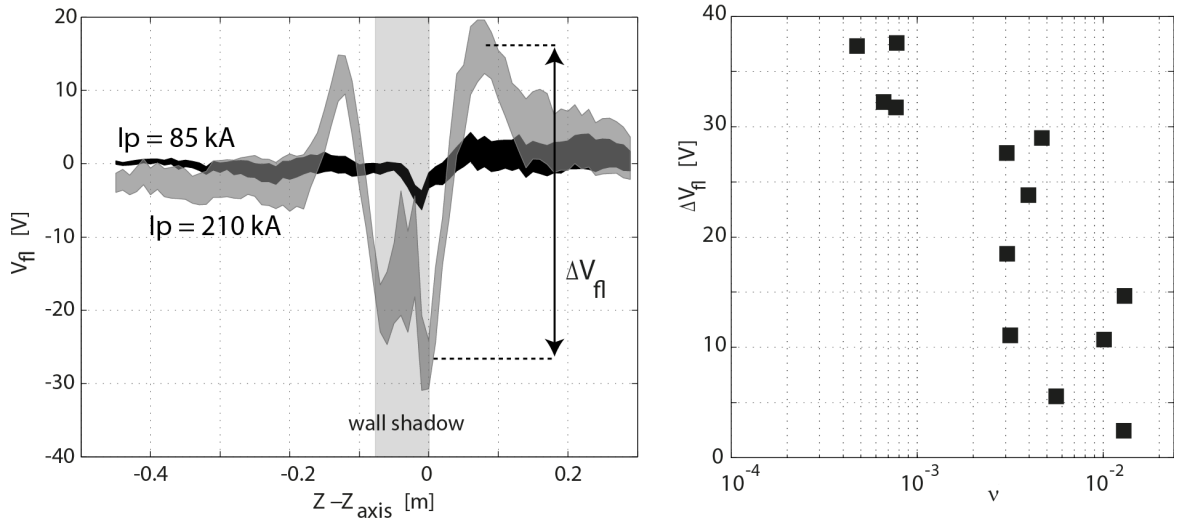


*FIG. 4: (left) Floating potential profile measured at the inner wall for $I_p$=85 kA and $I_p$=210 kA; (right) Floating potential drop $\Delta V_{fl}$ as a function of the normalized Spitzer collisionality.*

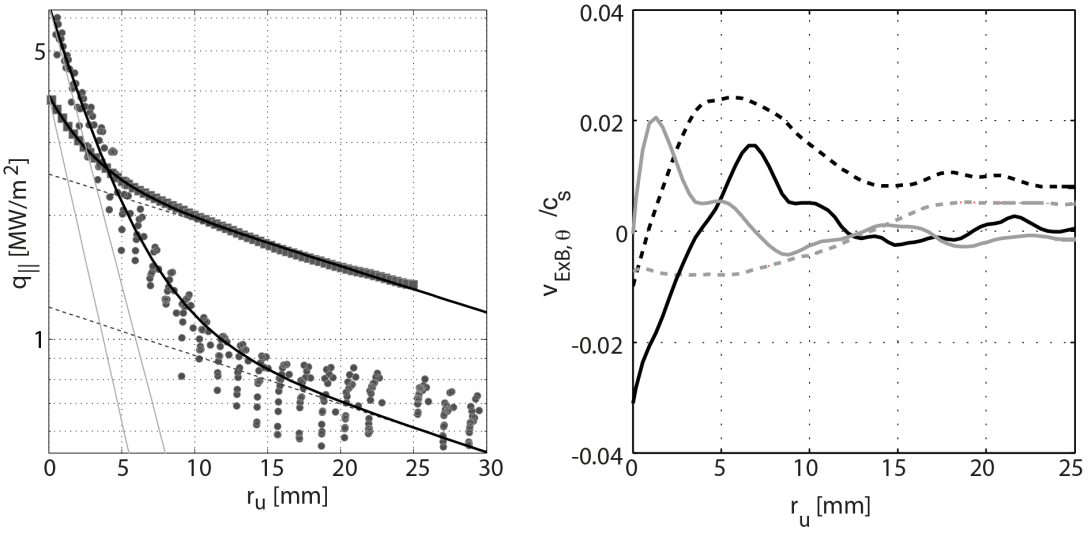


*FIG. 5: (left) Heat flux onto the limiter from GBS simulation (squares) and from IR thermography (circles) together with the fit with a sum of a short exponential (solid gray) and a long one (dashed black); (right) Radial profile of the poloidal component of the $E \times B$ velocity for both simulations: normal resistivity (black), large resistivity (gray) at the limiter (solid) and at the outboard midplane (dashed).*

## Global nonlinear simulations of the TCV SOL

To investigate the mechanisms leading to the heat deposition on the first wall, dedicated numerical nonlinear simulations of the SOL turbulence using the code GBS [13] have been performed for the first time with realistic TCV parameters [12]. By evolving the drift-reduced Braginskii equations, GBS allows for the self-consistent description of equilibrium and fluctuating quantities in a 3D geometry. Finite aspect ratio effects, ion temperature and magnetic shear are included in the simulations. These simulations feature open field lines only and the LCFS is set by the radial position of the plasma density and temperature source that mimics the injection of plasma from the core. Neutrals are not included in the simulations[14].

In a first simulation, the SOL of a TCV discharge (#49170) is modeled. It is a circular ($\kappa = 0$, $\delta = 0$) inboard-limited ohmic deuterium L-mode plasma with $I_p = 145$ kA and $B_\varphi = 1.45$ T. The plasma density at the LCFS ($n_{e,0} = 5 \times 10^{18}\,\mathrm{m}^{-3}$) and the electron temperature ($T_{e,0} = 25$ eV) are deduced from LP measurements at the limiter. The ion temperature at the LCFS is assumed to be $T_{i,0} = T_{e,0}$. These parameters set the normalized Spitzer resistivity to $\nu = 5.6 \times 10^{-3}$ and the dimensionless size of the system through the ion sound Larmor radius $\rho_s = \frac{c_{s,0}}{\omega_{ci}} = 5.9 \times 10^{-4}$ m. The edge safety factor $q_a = 3.2$, the magnetic shear $\hat{s} = 1.5$ and the inverse aspect ratio $\epsilon = 0.24$ are obtained from the magnetic reconstruction of the discharge. In a second simulation, the normalized resistivity has been increased by a factor 40. This choice is motivated by the fact that the heat flux carried out by the near SOL $\Delta P_{near} \propto T_{e,0}^{3/2} n_{e,0}^{-1} \propto \nu^{-1}$ as reported in [2] and confirmed with the results discussed in this paper (Fig3). Changing $\nu$

at fixed $\rho_s$ means that only the density $n_{e,0}$ is changed but not the electron temperature $T_{e,0}$. Figure 5(left) shows the resulting heat flux profile on one side the limiter and it is compared with the experimental profile. The simulated parallel heat flux radial profile has steep gradients in the near SOL and is well fit by a sum of two exponentials. The fitted values, $\lambda_{q,n}^{GBS} = 2.5$ mm and $\lambda_{q,f}^{GBS} = 35$ mm are in quantitative agreement with the experimental values: $\lambda_{q,n}^{IR} = 3.2$ mm, $\lambda_{q,f}^{IR} = 37$ mm (dashed black and solid gray lines in Fig.5(left)). Steep gradients in the near SOL are also visible at the LFS outboard midplane in the simulation. Nevertheless, the simulation is not able to reproduce the relative importance of the near SOL which is found to be much smaller than in the experiment: $\Delta P_{near}^{sim.} \simeq 1\,\mathrm{kW} \ll \Delta P_{near}^{exp.} \simeq 35\,\mathrm{kW}$. In contrast to experiment, the simulation at higher resistivity shows steeper gradients in the near SOL at the limiters, resulting in $\Delta P_{near}^{sim} \simeq 17$ kW. Nevertheless, steep gradients at the outboard midplan tend to vanish in the simulation. In a recent study, the $E \times B$ velocity shear is proposed as the driving mechanism for steepening the gradients, a signature of the near SOL [15]. This is consistent with our results: at low resistivity, the near SOL features steep gradients and the $v_{E\times B,\theta}$ profile is strongly sheared in the near SOL and at the limiter and the outboard midplane. At high resistivity, the $v_{E\times B,\theta}$ shear is much weaker in the near SOL at the outboard midplane and gradients have flattened (Fig. 5(right)).

## Conclusion and outlook

The near SOL of limited L-mode plasmas is characterized by steeper gradients than in the far SOL. It implies that the deposited heat flux density on the tiles is larger than expected and it might be a concern during the start-up phase of the plasma in ITER or in a reactor. For the first time, TCV results show that the strong gradients in the near SOL can be suppressed at high resistivity ($\nu \gtrsim 10^{-2}$) which corresponds to the transition of the SOL regime from Sheath-Limited to Conduction-Limited. Non-ambipolar currents at the limiter are measured in presence of the near SOL. Their amplitude is clearly correlated with the power in the near SOL. Global numerical simulations of the TCV SOL of limited plasmas have been carried out for the first time. Heat flux profiles at the limiters are also characterized by a near SOL component. Increasing the resistivity in the simulations tends to suppress the near SOL gradients at the LFS outbard midplane but not at the targets in contrast to experiment. It is conjectured that steep gradients are attributed to a strong radial shear of the $E \times B$ drift velocity. To confirm those results, additional simulations featuring open and closed magnetic field lines, neutral dynamics and different boundary conditions, will be run in the future. In addition, our results will be compared with the scaling of the main SOL parallel heat flux width.

## Acknowledgement

This work has been carried out within the framework of the EUROfusion Consortium and has received funding from the Euratom research and training programme 2014-2018 under grant agreement No 633053. The views and opinions expressed herein do not necessarily reflect those of the European Commission or of the ITER Organization.

# References

[1] KOCAN, M. et al., "Impact of a narrow limiter SOL heat flux channel on the ITER first wall panel shaping", Nucl. Fusion **55** (2015) 033019

[2] NESPOLI, F. et al., "Heat loads in inboard limited L-mode plasmas in TCV", J. Nucl. Mat. **463** (2015) 393-396

[3] HORACEK, J. et al., "Multi-machine scaling of the main SOL parallel heat flux width in tokamak limiter plasmas ", Plasma Phys. Control. Fusion **58** (2016) 074005

[4] GOLDSTON, R.J., "Theoretical aspects and practical implications of the heuristic drift SOL model", J. Nucl. Mat. **463** (2015) 397-400

[5] EICH, T., et al., "Scaling of the tokamak near the scrape-off layer H-mode power width and implications for ITER", Nucl. Fusion **53** (2013) 093031

[6] PITTS, R.A. et al., "The design of central column tiles for the TCV tokamak", Nucl. Fusion **39** (1999) 1433

[7] MAURIZIO, R. et al, "Infrared measurements of the heat flux spreading under variable divertor geometries in TCV", ECA **40A** (2016) P4.027

[8] BOEDO, J.A. et al., "Fast scanning probe for the NSTX spherical tokamak", Rev. Sci. Instrum. **80** (2009) 123506

[9] HERRMANN., A., " Limitations for Divertor Heat Flux Calculations of Fast Events in Tokamaks", ECA **25A** (2001) 2109 -2112.

[10] STANGEBY, P. C., "The Plasma Boundary of Magnetic Fusion Devices" (Bristol: Institute of Physics Publishing (2000).

[11] DEJARNAC, R. et al., "Understanding narrow SOL power flux component in COMPASS limiter plasmas by use of Langmuir probes", J. Nucl. Mater. **463** (2015) 381-384

[12] NESPOLI, F. et al., "Non-linear simulations of the TCV Scrape-Off Layer", submitted to Nuclear Material and Energy

[13] HALPERN, F.D. et al, "The GBS code for tokamak scrape-off layer simulations", J. Comp. Physics, **315**, (2016) 388-408 6

[14] WERSAL C. et al., "A first-principles self-consistent model of plasma turbulence and kinetic neutral dynamics in the tokamak scrape-off layer", Nucl. Fusion, **55**, 123014, (2015)

[15] HALPERN, F.D. et al, "Velocity shear, turbulent saturation, and steep gradients in the scrape-off layer of inner-wall linited tokamaks", submitted to Nuclear Fusion